CLM-R229

UKAEA

Report

THE CALCULATION OF SPECTRUM LINE EMISSION FROM PLASMAS

H. GORDON
H. P. SUMMERS
J. A. TULLY

CULHAM LABORATORY
Abingdon Oxfordshire

1982

C/18

Available from H. M. Stationery Office

£3.00

CLM-R 229

THE CALCULATION OF SPECTRUM LINE EMISSION FROM PLASMAS

I. Line Emission from low levels of ions

H Gordon*, H P Summers* and J A Tully‡

Culham Laboratory, Abingdon, Oxon, OX14 3DB, UK

(Euratom/UKAEA Fusion Association)

ABSTRACT

This is the first of a series of papers which will describe a number of Fortran computer programs and their associated data sets which will predict spectrum line emission from important species in fusion plasmas. The present work is concerned with the emission of line radiation by low lying excited states of ions. Three sets of plasma conditions are investigated, namely, the ionisation equilibrium plasma, the plasma developing in time and the plasma in a spatially inhomogeneous state.

The paper is divided into five sections. An introduction is presented in section 1. In sections 2 and 3 the theoretical outline is presented. Section 3 concentrates on the calculation of line emission and excited state populations and describes the atomic data required for that purpose. Section 3 describes the three sets of plasma conditions investigated. In section 4 the organisation of the programs and source data sets is described and finally, section 5 presents some results for illustration.

* Dept of Natural Philosophy, University of Strathclyde, Glasgow

‡ Observatoire de Nice, B.P. 252, 06007 Nice Cedex, France

ISBN 0 85311 113 8

1. Introduction

Emission of radiation by impurity species is a principal power loss mechanism of fusion plasmas. A major objective, therefore, is to monitor this emission and from theoretical modelling of the emission deduce overall radiative power loss, impurity abundance and other parameters of the plasma. The possibilities, both in theory and practice, for using spectral line emission from ions in the plasma to infer electron temperature, electron density and ion temperature have been widely investigated (c.f. McWhirter and Summers, 1982). The radiation can also yield information on the non-equilibrium state of the plasma, spatial or temporal, and on the presence of charge exchanging reactions in the plasma. The latter are particularly interesting since neutral beam injection is one of the favoured methods of energy input to the plasma. From the diagnostic point of view, then, the spectral emission by impurity species in the plasma can potentially be used as a signature for a wide variety of plasma compositions and conditions.

To support such a diagnostic program, it is necessary to have theoretical models for the plasma emission. Theoretical modelling of radiation emission requires a large amount of atomic physics data, particularly oscillator strengths, excitation and ionisation cross-sections and recombination coefficients. In recent years great effort has gone into providing this raw data of which there is now a very substantial amount. Consequently it is now possible to predict the emission of a large number of ions with reasonable accuracy. Our present objective is to assemble and make available a number of Fortran computer programs and associated data sets which permit prediction of spectrum line emission from important species in fusion plasmas under a range of conditions. This paper is envisaged as the first of a number of articles describing various aspects and developments of the programs

and data sets. The assembly and revision of the atomic data sets is an ongoing process.

The present work is concerned with the emission of line radiation by low lying excited states of ions. For such states it is assumed that the mechanism of line emission by a particular ion is principally excitation from the ground state (or possibly a metastable state of that ion), followed ultimately by spontaneous emission. This does not preclude collisional redistribution of electrons among the low excited states but does imply that populating of the states either by recombination or charge exchange may be neglected. This will be the subject of a later paper. The intensity of a line depends, therefore, on the ground state population of that ion. It is assumed that timescales are sufficiently long for excited populations to be relaxed relative to the instantaneous ground population. The populations of ground states of ions (which are to a good approximation the stage abundances) relax much more slowly relative to other ionisation stage abundances, so the stage abundances may take ionisation equilibrium values or take non-equilibrium values depending upon the type of plasma.

The paper is divided into five sections. In sections 2 and 3 the theoretical outline is presented. Section 2 concentrates on the calculation of line emission and excited state populations, and describes the variety of atomic data required for that purpose. Section 3 describes the three broad sets of plasma conditions addressed here, namely, the ionisation equilibrium plasma, the plasma developing in time, and the plasma in a spatially inhomogeneous state. In section 4 the organisation of the programs and source data sets is described and flow diagrams given of their interrelations. In section 5, some results are given for illustration. Acquisition of atomic data and uncertainties in the results are explored for these illustrative cases. Operation of the programs and user data provision is

described in an appendix.

2. The Calculation of Populations

2.1 Population balance

In an optically thin plasma composed of impurity ions of low number density in a fully ionised hydrogen plasma, the principal processes establishing the populations of low excited states $A^{+z}(i)$ of an ionisation stage, A^{+z} of element A are

(a) Collisional excitation and de-excitation by electrons

$$A^{+z}(i) + e \rightleftarrows A^{+z}(j) + e \qquad 1.$$

(b) Collisional excitation and de-excitation by protons.

$$A^{+z}(i) + p \rightleftarrows A^{+z}(j) + p \qquad 2.$$

(c) Spontaneous emission of radiation

$$A^{+z}(j) \longrightarrow A^{+z}(i) + h\nu \qquad 3.$$

In the present paper we neglect recombination processes and processes of inner shell ionisation leaving the ion in excited states. This will be treated in later work. The equations determining the populations N_i of the states $A^{+z}(i)$ are

$$\frac{dNi}{dt} = \sum_{j>i} (Ne\, q^{(e)}_{j\to i} + N_p\, q^{(p)}_{j\to i} + A_{j\to i})N_j + \sum_{j<i} (Ne\, q^{(e)}_{j\to i} + Np\, q^{(p)}_{j\to i})N_j$$

$$- \left(\sum_{j>i} (Ne\, q^{(e)}_{i\to j} + N_p\, q^{(p)}_{i\to j}) + \sum_{j<i} (Ne\, q^{(e)}_{i\to j} + Np\, q^{(p)}_{i\to j} + A_{i\to j}) \right) N_i \qquad 4.$$

The A's denote Einstein coefficients, the $q^{(e)}$ electron collisional rate coefficients, and the $q^{(p)}$ proton rate coefficients. Ne is the electron density and Np the proton density. Since the excited populations are in quasi static equilibrium with the ground population on timescales with which we are concerned, putting $n_i = \frac{Ni}{N_1}$ and $\frac{dNi}{dt} = 0$ for $i \neq 1$, a set of simultaneous equations for the Ni are obtained.

The solution of these may be written as

$$n_i = F_i(Ne, Np, Te) \quad i \neq 1. \qquad 5.$$

This assumes that there are no metastable states present with relaxation times comparable with the ground state. Such metastable states, if present, should be treated as further effective ground states. For a single metastable state labelled by i = 2, in addition to the ground state, i = 1, equation 5 is replaced by,

$$n_i = f_i(Ne, Np, Te) + g_i(Ne, Np, Te)n_2 \quad i \neq 1,2 \qquad 6.$$

where n_2 must be deduced from ionisation balance and dynamical considerations in general if our timescales are shorter than metastable relaxation times. Evidently

$$F_i = f_i(Ne, Np, Te) + g_i(Ne, Np, Te)\, F_2(Ne, Np, Te) \quad i \neq 2 \qquad 7.$$

We shall define the emissvity $P_{i\to j}$ as the number of photons emitted per A^{+z} ion per cm^3 per sec. Since it is a good assumption that the overall population of an ionisation stage is concentrated overwhelmingly in the ground (and metastable levels) the emissivity is

$$P_{i\to j}(A,z) = A_{i\to j}\, F_i \qquad 8.$$

with no metastables present, and

$$P_{i\to j}(A,z) = A_{i\to j}\left(\frac{f_i + g_i\, n_2}{1 + n_2}\right) \qquad 9.$$

when there is a single metastable state. The reliability of the application of these expressions depends on having a sufficiently complete set of states i included in equations 4. As specific applications will severely restrict the total number of states included (due to lack of data) systematic errors occur in the calculated emissivities. These errors are discussed in section 5.

The formulae for the line emissivities must be implemented in a particular angular momentum coupling scheme for the emitting ion states. At low z, since we are concerned with low excited states, with small fine structure splitting, the populations are taken to be those of LS coupled terms. Usually the metastable terms if they exist are the lowest states of alternative spin systems

from that of the ground state. At high z the populations of the separate LSJ levels must be considered. At low electron density, fine structure levels of the ground term (if present) are metastable in this case.

For comparison of line emission from ions in different stages of ionisation, the emissivity in a particular line per impurity species atom in any stage, per cm^3 per sec is required. We write

$$P_{i\to j}(A) = P_{i\to j}(A,z)\,\frac{N(A,z)}{N(A)} \qquad 10.$$

The fractional abundances of the ionisation stages $\frac{N(A,z)}{N(A)}$ required for this formula depend on the dynamic state of the plasma in general, and may be of independent interest. The possibilities are examined in section 3.

2.2 Electron collisions

The electron collisional excitation and deexcitation rate coefficients $q^{(e)}_{i\to j}$ and $q^{(e)}_{j\to i}$ of equations (4) are required. The accuracy of these rates normally is the determining factor in the accuracy of calculated emissivities. Ab initio cross-section calculations are not made here. For this work our objective has been to compile, into suitable data sets, good accuracy collision cross-section calculations from a variety of sources. The literature on such calculations is very large. Four approximations have been widely and successfully applied, namely, close-coupling, distorted wave, Coulomb-Born and variants of the Bethe approximation for dipole allowed excitations. The first two have the generality and accuracy required for the present work. The Coulomb-Born method refers to the z-scaling calculations of Sampson and co-workers and derives from the earlier work of Burgess et al. (1970). There are now a substantial number of such calculations published of good accuracy, which have the additional advantage of describing transitions along whole isoelectric sequences. These results provide a valuable supplement when close-coupling and distorted wave data are not available. Approximations such as the impact parameter method are useful when the others are lacking, and sufficiently reliable oscillator strangths can be obtained. Many of the

published distorted wave calculations originate from the codes developed at University College, London (Eissner et al., 1974). Two close coupling codes are widely used, namely, the R-matrix code originating at Queens University, Belfast (Burke et.al., 1971; Henry, 1981) and the Impact code of University College, London (Crees et.al. 1978). We use data from all these methods.

Numerical results from collision calculations are presented in a number of different ways. These include the collision cross-section $Q_{i\to j}$, the collision strength Ω_{ij}, the rate parameter γ_{ij}, the excitation rate coefficient $q^{(e)}_{i\to j}$ and the deexcitation rate coefficient $q^{(e)}_{j\to i}$ where j denotes the upper and i the lower level. The following relations exist between these quantities

$$
\begin{aligned}
q^{(e)}_{j\to i}\,(Te) &= e^{\Delta E_{ij}/kTe}\ \frac{w_i}{w_j}\ q^{(e)}_{i\to j}(Te) \\
&= 8.63\times 10^{-6}\ \frac{1}{w_j Te^{1/2}}\ \gamma_{ij}(Te) \\
&= 8.63\times 10^{-6}\ \frac{1}{w_j Te^{1/2}} \int_0^\infty \Omega_{ij}(\varepsilon) e^{-\varepsilon/kTe}\ d(\varepsilon/kTe) \qquad 11.
\end{aligned}
$$

where ΔE_{ij} is the transition energy in Rydbergs, ε is the free electron kinetic energy relative to the level j of the ion in Rydbergs. w_i and w_j are statistical weights of states i and j respectively. Te is measured in electron-volts.

The data sets compiled here contain tabulated cross-sections stored in three forms

(a) $\Omega_{ij}(\varepsilon)$ for $\varepsilon = \varepsilon_o, - - -, \varepsilon_n$

(b) $\lim_{z\to\infty} z^2\Omega_{ij}(\overline{\varepsilon})$ for $\overline{\varepsilon} = \lim_{z_1\to\infty} \frac{\varepsilon}{z_1^2} = \overline{\varepsilon_1}, - - -, \overline{\varepsilon_n}$

(c) $\gamma_{ij}(Te)$ for $Te = T_1, - - -, T_n$

In (b), z_1+1 is the ion charge. The infinite z results of Sampson and co-workers may be converted to data of type (a) for a specific member of an isoelectronic sequence given an effective charge z_{eff} for that member.

Collision strengths often show resonant behaviour below the thresholds for the opening of new channels. In such cases the data sets used here are of thermally averaged collision strengths which we refer to as the rate parameter $\gamma(Te)$.

A numerical code is used to obtain excitation and deexcitation rates from these data sets for any electron temperature by quadratures, interpolation and extrapolation, as described below.

Forms (a) and (b)

Consider the deduction of the rate parameter $\gamma(Te)$ for arbitrary Te from data of type (a) or (b). There are three separate categories:

(i) Dipole transitions

The collision strength takes the approximate form

$$\Omega(\varepsilon) = -C_2 \ln \xi + C_o + C_1 \xi \text{ where } \xi = \frac{\Delta E}{\varepsilon+\Delta E} \qquad 12.$$

with ΔE the transition energy. We wish to exploit this form for interpolation and extrapolation of Ω between tabulated values. C_2 is given explicitly in terms of the absorption oscillator strength $f_{i\to j}$ by

$$C_2 = \frac{-4\, w_i\, f_{i\to j}}{(\Delta E/I_H)} .$$

C_o and C_1 are obtained by fitting to the tabulated data in each interval $\varepsilon_k \leq \varepsilon \leq \varepsilon_{k+1}$. The contribution of the range $\varepsilon_k \leq \varepsilon \leq \varepsilon_{k+1}$ to the resulting γ is

$$\int_{\varepsilon_k/kTe}^{\varepsilon_{k+1}/kTe} \Omega(\varepsilon) e^{-\varepsilon/kTe}\, d(\varepsilon/kTe)$$

$$= C_o(e^{-\varepsilon_k/kTe} - e^{-\varepsilon_{k+1}/kTe}) + (C_1\frac{\Delta E}{kTe} - C_2)e^{\Delta E/kTe}\{E_1(\frac{\varepsilon_k+\Delta E}{kTe}) - E_1(\frac{\varepsilon_{k+1}+\Delta E}{kTe})\}$$

$$- C_2\{e^{-\varepsilon_k/kTe} \ln(\frac{\Delta E}{k+\Delta E}) - e^{-\varepsilon_{k+1}/kTe} \ln(\frac{\Delta E}{\varepsilon_{k+1}+\Delta E})\} \qquad 13.$$

This immediately yields suitable expressions also for the contribution from the ranges $0 \leq \varepsilon \leq \varepsilon_o$ and $\varepsilon_n \leq \varepsilon \leq \infty$.

(ii) Non-dipole transitions - no spin change

The collision strength takes the approximate form

$$\Omega(\varepsilon) = C_o + C_1 \xi \qquad 14.$$

with ξ defined as in equation 12.

The contributions to γ from each interval follow from equation 13 by setting $C_2 = 0$.

(iii) Non-dipole transitions - spin change

Relativistic terms in the Hamiltonian cause LS coupling breakdown which can lead to a dipole component in apparent spin change transitions and hence a contribution to γ of type (i). Here we are concerned with the non-dipole pure exchange contribution. The collision strength takes the approximate form

$$\frac{1}{\xi^2}\ \Omega(\varepsilon) = C_o + C_1 \xi \qquad 15.$$

with ξ defined as in equation 12.

C_o and C_1 are obtained as above in each tabular interval $\varepsilon_k \leq \varepsilon \leq \varepsilon_{k+1}$.

The contribution from this range to the resulting γ is

$$\int_{\varepsilon_k/kTe}^{\varepsilon_{k+1}/kTe} \Omega(\varepsilon) e^{-\varepsilon/kTe}\, d(\varepsilon/kTe)$$

$$= e^{\Delta E/kTe}\{C_o(\frac{\Delta E}{kTe})^2\{E_2(\frac{\varepsilon_k+\Delta E}{kTe}) - E_2(\frac{\varepsilon_{k+1}+\Delta E}{kTe})\} + C_1(\frac{\Delta E}{kT})^3\{E_3(\frac{\varepsilon_k+\Delta E}{kTe}) - E_3(\frac{\varepsilon_{k+1}+\Delta E}{kTe})\}\} \qquad 16.$$

Again contributions from $0 \leq \varepsilon \leq \varepsilon_o$ and $\varepsilon_n \leq \varepsilon \leq \infty$ follow immediately.

The confidence which can be placed in these formulae when the mean thermal energy kTe $\geq \varepsilon_n$ is not great. It has been pointed out by Tully that although the parameterising used here in (i), (ii), and (iii) is most appropriate for mapping out the full range of the collision strength, the approach to the high energy limit, $\xi = 0$, can be rapidly varying in some cases. In general we shall have only a small number of tabular values available, normally in the vicinity of excitation threshold.

Form (c)

The tabulated rate parameters γ have simply to be interpolated and/or extrapolated in this case. A rather larger number of tabular values are generally available and it proves most satisfactory to use cubic spline interpolation of $\ell n\ \gamma$ with ℓn Te as the independent variable. The latitude in end conditions of the splines can be used to fit smoothly onto appropriate asymptotic forms. For extrapolation to low electron temperature, zero curvature at the first knot is imposed with constant gradient projection. For extrapolation to high electron temperature the spline is adjusted at the end knot to give first and second derivative continuity. This determines the asymptotic parameters C_o and C_1 in the formula derived from equations (13) and (16) by letting $\varepsilon_k \to 0$ and $\varepsilon_{k+1} \to \infty$. These are

$$(i)\quad \gamma = C_o + \left[C_1\left(\frac{\Delta E}{kTe}\right) - C_2\right] e^{\Delta E/kTe}\, E_1\left(\frac{\Delta E}{kTe}\right) \qquad 17.$$

$$(ii)\quad \gamma = C_o + C_1\left(\frac{\Delta E}{kTe}\right) e^{\Delta E/kTe}\, E_1\left(\frac{\Delta E}{kTe}\right) \qquad 18.$$

$$(iii)\quad \gamma = e^{\Delta E/kTe}\left[C_o\left(\frac{\Delta E}{kTe}\right)^2 E_2\left(\frac{\Delta E}{kTe}\right) + C_1\left(\frac{\Delta E}{kTe}\right)^3 E_3\left(\frac{\Delta E}{kTe}\right)\right] \qquad 19.$$

The derivative conditions follow immediately from these expressions.

2.3 Proton collisions

Impact of charged heavy particles can be effective in causing transitions between ionic states in certain circumstances. For hydrogen plasmas with low impurity content, only impact of hydrogen nuclei needs to be taken into account. Without loss of generality, we shall refer only to proton collisions here. The same procedures apply for collisions involving deuterium or tritium nuclei apart from adjustment of the mass factor. Proton collisions are of comparable or greater importance than electron collisions when the transition energy ΔE is sufficiently small. This is the case (a) for electric quadrupole transitions between fine structure levels belonging to the same LS term and (b) for electric dipole transitions between nearly degenerate ℓ states belonging to the same principal quantum number. The latter relate to highly excited states, but the former are particularly important for determining the population structure low lying levels.

Semi-classical impact parameter theory is appropriate to such collisions, and a number of applications have been made based mostly on the work of Alder et.al. (1956). Following Alder et.al., the cross-section for an electric 2^{λ}-multipole transition, due to proton impact, may be written in first order perturbation theory as

$$Q^{\lambda}_{i\to j}(E_i) = \left(\frac{I_H}{E_i}\right)\left(\frac{m_p}{m_e}\right)\left(\frac{a_o}{a}\right)^{2\lambda-2}\overline{B}^{\lambda} f^{\lambda}(\xi)\, a_o^{\,2} \qquad 20.$$

and the transition probability for a collision trajectory of impact parameter is

$$P^{\lambda}_{i\to j}(R) = 4\left(\frac{m_p}{m_e}\right)\frac{1}{z}\left(\frac{a_o}{a}\right)^{2\lambda-1}\overline{B}^{\lambda}\sin^4\frac{\nu}{2}\,\frac{df^{\lambda}(\xi,\nu)}{d\Omega} \qquad 21.$$

The impact parameter, R, and angle of deflection ν are related by

$$R = z\, a_o \left(\frac{I_H}{E_i}\right)\cot\frac{\nu}{2} \qquad 22.$$

and z is the target ion charge number.

The collision is parameterised by a and ξ which take the form

$$a = z a_o \left(\frac{I^2_H}{E_i E_j}\right)^{\frac{1}{2}} \quad , \quad \xi = z\sqrt{\frac{m_p}{m_e}} \left| \sqrt{\frac{I_H}{E_i}} - \sqrt{\frac{I_H}{E_j}} \right| \qquad 23.$$

Case (a) Electric quadrupole transitions

The functions $f^{(2)}(\xi)$ and $\frac{df^{(2)}(\xi,\nu)}{d\Omega}$ have been tabulated by Alder et.al. (1956). Their results have been applied to the atomic case by a number of authors. We use here a program developed by Bely (see Bely & Faucher, 1970). Since there are slight variations between different authors' work, it is worthwhile expanding on some details of the Bely calculation. $\overline{B}^{(2)}$ is related to the Einstein A coefficient by

$$\overline{B}^{(2)} = \frac{600}{\pi} \frac{a_o}{\alpha^6 c} \frac{w_j}{w_i} A_{j\to i} \left(\frac{I_H}{\Delta E}\right)^5 \qquad 24.$$

For small impact parameters P(R) can exceed unity. The states i and j are then strongly coupled and perturbation theory breaks down. Bely modifies the transition probability in equation (21) so that at small R it does not exceed $\frac{1}{2}$. Thus he takes

$$Q^{(2)}_{i\to j}(E) = \int_0^\infty \frac{P(R)}{\left[1 + \frac{P(R)}{4}\right]^2} 2\pi R dR \qquad 25.$$

The transition probability here vanishes as $R \to o$. Landman and Brown (1979) assume a constant probability for the inner region, defined as that within a cut-off impact parameter R_o equal to the classical distance of closed approach. For both Landman and Bely the cross-sections satisfy the usual quadrupole selection rule, namely $J = 0 \not\to J = 1$.

Sahal-Brechot (1974) assumes that in the close coupling region transitions to all fine structure components are equally probable so that the cross-section contributions from the inner region are proportional to the statistical weights of the final states. Consequently Sahal-Brechot obtains a non-zero value for $J=0 \to J=1$.

Case (b) Electric dipole transitions

For completeness, we describe this case here only briefly since it is not of importance in the present work.

The theory of Alder et.al. has been applied to this case by Burgess (1964) (see also, Burgess and Summers (1976)). We use Burgess' method to describe both electron and proton impact excitation of transitions between highly excited states for which more reliable cross-sections are not available.

The functions $f^{(1)}(\xi)$ and $\frac{df^{(1)}(\xi,\nu)}{d\Omega}$ are essentially those denoted as Y and X by Burgess and Summers. Note that in the dipole case

$$\overline{B}^{(1)} = \frac{9}{2\pi} \frac{a_o}{\alpha^4 c} \left(\frac{I_H}{\Delta E}\right)^3 \frac{w_j}{w_i} A_{j \to i} \qquad 26.$$

2.4 Spontaneous emission coefficients and energy levels

Configuration assignment and LSJ are used for level labelling since these are most appropriate to the low levels with which we are concerned. This does not preclude spontaneous transitions arising from a breakdown of LS coupling or configuration mixing. We attempt to include all relevant transition probabilities in our calculations. Einstein A values and energy levels are drawn from the literature where available. Where there are serious omissions, we supplement with our own calculations using the UCL Superstructure code (see Eissner et.al., 1974) and the code of Cowan (Cowan, 1968; Cowan and Griffin, 1976). These are both multiconfiguration codes incorporating relativistic corrections. In using results derived from large structure computations when configuration mixing is strong, configuration and parent assignment can be ambiguous. In those cases we have accepted the level labelling of the computer codes. Usually the wave functions from the structure calculation are entered directly into the

associated collision calculation and so consistency is maintained between the spontaneous emission and collisional rate coefficients.

3. Calculation of the State of Ionisation

3.1 Equilibrium ionisation balance

In local statistical equilibrium, the fractional abundances of impurity ions in a hydrogen plasma $\frac{N(A,z)}{N(A)}$ depend principally on electron temperature and more weakly on electron density. It is convenient to view this equilibrium as a balance between recombination events and ionisation events. We describe the effective electron-ion recombination rate from $A^{+(z+1)}$ to A^{+z} by the 'collisional-dielectronic recombination coefficient', $\alpha_{cd}(A,z+1)$, so that the number of recombinations per cm^3 per sec is

$$N_e\, N(A,z+1)\, \alpha_{cd}(A,z+1) \qquad 27.$$

Likewise the effective collisional ionisation rate from A^{+z} to $A^{+(z+1)}$ is described by the 'collisional dielectronic ionisation coefficient', $S_{cd}(A,z)$ so that the number of ionisations per cm^3 per sec is

$$N_e\, N(A,z)\ \ S_{cd}(A,z) \qquad 28.$$

The coefficients α_{cd} and S_{cd} depend on N_e and T_e in general (N_p and T_p may be neglected), but provided the density is not too large, S_{cd} is almost independent of N_e, and α_{cd} approaches its low density limit. In equilibrium in a plasma with thermalised electrons, multiple ionising events are rare and so

$$\frac{N(A,z)}{N(A,z+1)} = \frac{\alpha_{cd}(A,z+1)}{S_{cd}(A,z)} \qquad 29.$$

from which the fractional abundances $\frac{N(A,z)}{N(A)}$ can be computed.

α_{cd} and S_{cd} are composite coefficients which take account of the various individual processes which link ionisation stages $A^{+(z+1)}$ and A^{+z}, and are the result of elaborate calculation. We use the program developed by

Summers (1974) in order to generate α_{cd} and S_{cd} for hydrogen-like to argon-like ions.

When using ionisation and the recombination rates, it should be noted that some of the available data for processes such as direct ionisation rates have large uncertainties. Likewise detailed calculations for specific ions selectively improve particular coefficients. It is desirable therefore to permit substitution of some rate coefficients with alternatives and to allow scaling or adjustment of selected values.

3.1.1 The ionisation coefficient

This has been reviewed in some depth by Burgess et.al. (1977). There is considerable uncertainty in the direct ionisation rate of ground state ions. Simple but approximate formulae tend to be widely used. Further, the method for the proper inclusion of excitation to auto-ionising levels and inner shell ionisation has to be considered.

The collisional dielectronic ionisation coefficient is composed of direct ionisation from the ground state and stepwise ionisation via excited states. The stepwise part is the origin of the density dependence of the coefficient. We shall call this S^{I}_{cd}. For a particular ion (i.e. A and z) showing explicitly the dependence of the coefficients on N_e and T_e, to a good approximation

$$S^{I}_{cd}(N_e,T_e) = S_{cd}(N_e,T_e) - S_{cd}(o,T_e) \qquad 30.$$

whereas the direct part

$$S^{D}(T_e) = S_{cd}(o,T_e) \qquad 31.$$

is independent of N_e. The direct part is composed of ionisation from the outer shell, inner shells and excitation to autoionising levels leading to ionisation

$$S^{D}(T_e) = \sum_i S(\chi_i,\zeta_i,T_e) + \sum_i q^{A}(j,T_e) \qquad 32.$$

where $S(\chi_i,\zeta_i,T_e)$ denotes ionisation from the shell i of ionisation

potential χ_i and number of equivalent electrons ζ_i. $q^A(j,T_e)$ denotes ionisation occurring through excitation to level j which is assumed to autoionise with branching ratio unity. The treatment of autoionisation is often accomplished most effectively by combining it with the shell ionisation rates and adjusting the χ_i and ζ_i. So alternatively we write

$$S^D(T_e) = \sum_i S(\chi_i', \zeta_i', T_e) \qquad 33.$$

Some combination of the two strategies may sometimes be most appropriate.

The collisional dielectronic procedure of Summers (1974) uses ECIP approximation for $S(\chi_i,\zeta_i,T_e)$ and also evaluates S_{cd}^I. It computes dipole contributions to q^A for ionisation of first period isoelectronic sequences and uses the Coulomb-Born results of Bely (1968) for second period ionisation. As pointed out by Burgess et.al. (1977), non dipole contributions to the autoionisation should be included for first period ionisation. Finally, for high z improvement of ionisation potentials can also be made. Alternative choices for $S(\chi_i,\zeta_i,T_e)$ are ECIP (Burgess, 1964), SEF (Seaton, 1964; Lotz, 1967) and infinite z Coulomb-Born (see Golden and Sampson, 1977). We provide the following alternatives:

1. S_{cd} - Summers (1974) without autoionisation
2. S_{cd} - " " with autoionisation
3. S^D only - ECIP with input of χ's, ζ's and optional autoionisation data
4. S^D only - SEF with input of χ's, ζ's and optional autoionisation data
5. S_{cd}^I from Summers (1974) with (3) for direct ionisation
6. S_{cd}^I " " " " (4) " " "

3.1.2 The recombination coefficient

We use the data of Summers (1974) for the collisional dielectronic recombination coefficient α_{cd}. Modification of these values is less easy than for S_{cd} insofar as a substantial part of the effective recombination occurs through highly excited states. Some revision of the zero density recombination rate is warranted for certain ions due to improved calculations of secondary autoionisation, alternative Auger channels, better cross-sections etc. Further revisions are also likely as the treatment of metastable states in recombination improves. For the present we provide two alternatives:

1. α_{cd} - Summers (1974).

2. Scaled α_{cd} - scaling factor F(z,config) supplied as data.

3.2 A time dependent ionisation model

The collisional dielectronic ionisation and recombination coefficients S_{cd} and α_{cd} can be used to calculate the fractional ionisation stage abundances in non-equilibrium situations, provided conditions do not depart too far from ionisation balance. Their use will break down if multiple ionisation becomes significant. We develop a simple time dependent, spatially homogeneous model in this section.

The model requires the electron density and electron temperature as functions of time. This is specified as a set of tabular values

$$T_e(t_i) \quad : \quad i=1,---,m$$

$$N_e(t_i) \quad : \quad i=1,---,m \ .$$

From the calculations of section 3.1 the coefficients α_{cd} and S_{cd} are obtainable at the same set of times.

These tabular values can then be interpolated over the whole range $t_1 \leq t \leq t_m$ using splines. The differential equations for the time dependent stage abundances, where we now write $N(z) \equiv N(A,z)$, $\alpha_{cd}(z) \equiv \alpha_{cd}(A,z)$ and $S_{cd}(z) \equiv S_{cd}(A,z)$, are

$$\frac{dN(o)}{dt} = N_e \left[- S_{cd}(o)\, N(o) + \alpha_{cd}(1)\, N(1) \right]$$

$$\frac{dN(z)}{dt} = N_e \left[S_{cd}(z-1)\, N(z-1) - (\alpha_{cd}(z) + S_{cd}(z))\, N(z) + \alpha_{cd}(z+1)\, N(z+1) \right] \qquad 34.$$

$$\frac{dN(z_o)}{dt} = N_e \left[S_{cd}(z_o-1)\, N(z_o-1) - \alpha_{cd}(z_o)\, N(z_o) \right]$$

The solution of these equations with specified abundances at time $t = t_o$ yield the fractional abundances at each time $t_o, ----, t_m$.

3.3 A time independent spatially inhomogeneous model

The plasma in this case is assumed stationary in time, but spatially inhomogeneous. We consider the combination of diffusion and ionisation processes in a section of cylindrical symmetry with no azimuthal variation. This can simulate a θ-pinch section, or with suitable diffusion coefficients taking account of toroidal effects, a section of the torus of a Tokamak. Letting ρ be the radial coordinate and omitting the element label A, the stage abundances are obtained from the differential equations

$$\frac{1}{\rho}\frac{d}{d\rho}\left(\rho v(z)\, N(z)\right) = N_e \left(S_{cd}(z-1) N(z-1) - (S_{cd}(z) + \alpha_{cd}(z)) N(z) + \alpha_{cd}(z+1)\, N(z+1) \right)$$

for $z = o, ---, z_o$ with $\alpha_{cd}(o) = S_{cd}(-1) = \alpha_{cd}(z_o+1) = S_{cd}(z_o) = 0$ 35.

The radial coordinate ρ satisfies $o \leq \rho \leq \rho_m$ and $v(z)$ denotes the radial velocity of the ion A^{+z}. We write

$$v(z) = f(z) - g(z)\, \frac{1}{N(z)}\, \frac{d(N(z))}{d\rho} \qquad 36.$$

so that for $\rho \neq o$ the equations become

$$f(z)\,N(z) + \rho\frac{d}{d\rho}(f(z)\,N(z)) - g(z)\frac{dN(z)}{d\rho} - \rho\frac{d}{d\rho}\left(g(z)\frac{dN(z)}{d\rho}\right)$$

$$= \rho N_e\left\{S_{cd}(z-1)\,N(z-1) - (S_{cd}(z)+\alpha_{cd}(z)\,N(z) + \alpha_{cd}(z+1)\,N(z+1)\right\} \qquad 37.$$

while at $\rho = o$ the equations reduce to

$$f(z)\,N(z) - g(z)\frac{dN(z)}{d\rho} = o$$

$$2N(z)\frac{df(z)}{d\rho} - 2g(z)\frac{d^2N(z)}{d\rho^2} - 2\frac{dg(z)}{d\rho}\frac{dN(z)}{d\rho} = N_e\left\{S_{cd}(z-1)\,N(z-1) - (S_{cd}(z)+\alpha(z))\,N(z) + \alpha_{cd}(z+1)\,N(z+1)\right\} \qquad 38.$$

Note that we also require

$$f(z)\Big|_{\rho=o} = \frac{dN(z)}{d\rho}\Big|_{\rho=o} = \frac{dg(z)}{d\rho}\Big|_{\rho=o} \qquad 39.$$

On summation over the ionisation stages, zero net flux through any cylindrical surface is obtained as required. That is

$$\rho\sum_{z=o}^{z_o}\left\{f(z)\,N(z) - g(z)\frac{dN(z)}{d\rho}\right\} = o \qquad 40.$$

The model requires the electron density, electron temperature, proton density, proton temperature and a velocity profile to be input as functions of radial position. This is achieved by introducing a set of tabular values

$T_e(\rho_i)$: $i=1,---,m$ with $\rho_1=o$

$N_e(\rho_i)$: ---------

$T_p(\rho_i)$: ---------

$N_p(\rho_i)$: ---------

$v(\rho_i)$: ---------

with $v(o)=o$ and $\frac{dT_e}{d\rho} = \frac{dN_e}{d\rho} = \frac{dT_p}{d\rho} = \frac{dN_p}{d\rho} = o$ at $\rho=o$.

As in section 3.2, the coefficients α_{cd} and S_{cd} are obtainable at the same set of positions. These sets of tabular values are interpolable over the whole range $o \leq \rho \leq \rho_m$ using splines. The model requires the specification of the functional forms of the diffusion velocities v(z). We permit a range of options, namely

$$
\begin{aligned}
f(o) &= a(o)v \\
g(o) &= d(o) \times 6.739^{16} \frac{T_p}{N_p} \\
f(z) &= a(z)v + 4.03^{-8} \left(\frac{b(z)}{T_p^{\frac{1}{2}}} \frac{dN_p}{d\rho} + c(z) \frac{N_p}{T_p^{3/2}} \frac{dT_p}{d\rho} \right) \\
g(z) &= 4.03^{-8} d(z) \frac{N_p}{T_p^{\frac{1}{2}}}
\end{aligned}
\qquad 41.
$$

Where the a(z), b(z), c(z), d(z) are independent of ρ and are specified for each ion $z=o,---z_o$ and are of order unity. The model is completed by specification of the ionisation stage fractional abundances at the boundary $\rho=\rho_m$.

Instead of a solution for the fractional abundances at each radial position, the stage abundances for specified neutral inward flux at $\rho=\rho_m$ may be obtained.

4. Computational Organisation

The principal program unit is called MAIN, and is organised into three sections. In section 2, an ion is specified together with electron and proton temperatures and densities. The program then evaluates the populations of the low lying excited states of the ion relative to its ground level population. Two principal subroutines are employed, namely ELRAT which computes electron excitation and de-excitation rates and PRAT which computes proton collision rates. Both of these subroutines require preassembled cross-section data.

MAIN accesses the appropriate data sets, assembles the collisional radiative coefficient matrix through calls to ELRAT and PRAT and executes a matrix inversion, MATINV, to determine the relative populations.

In general, the line emission from several ionisation stages on an absolute basis is required. Section 1 of MAIN calculates the fractional abundances of the selected ionisation stages depending upon the choice of model. Subroutine ION3 is first called to obtain relevant collisional dielectronic recombination and ionisation coefficients and the fractional abundances in ionisation balance. Then optionally ION4 is called to provide the time dependent abundances or ION5 to provide spatially non-equilibrium abundances. ION3 can make use of alternative ionisation and recombination rate coefficient options. The routines RSEF and RECIP provide the Seaton semiempirical and Burgess ECIP ionisation rate coefficients respectively (cf. Burgess et.al. 1977).

With stage abundances established, section 2 of MAIN is entered recursively in order to obtain the excited state populations for each ionisation stage.

Once the populations are determined section 3 of MAIN is entered recursively to provide the emissivities for each emitted spectrum line for each ion of the set. At each stage of the calculation, output of useful intermediate results is possible. This can be in both graphical and numerical form.

A number of sets of atomic data must be accessed during the calculation. Proton differential cross-section data for quadrupole transitions required by the subroutine PRAT is provided in the data set PROTDATA. Data for ELRAT can be provided either

(1) for a specific ion or (2) in a general purpose form usable for arbitrary z (not yet implemented). The data for a specific ion is assembled in partitioned data sets. The partitioned data set name reflects the element title while the member name describes the ion, e.g. TIDATA(TI19) denotes the data set for titanium and the member for Ti^{+19}. A further member contains the stacked data for all the available stages arranged sequentially in increasing ion charge. For the titanium case this member is simply TIDATA(TITANIUM).

The subroutine ION3 requires interpolable data sets of collisional dielectronic recombination and ionisation rate coefficients. These are titled ACDSCD1 and ACDSCD2 for cases 1,5,6 and case 2 respectively (section 3.11). A further data set of ionisation potentials and autoionisation data may also be required entitled IPAXDATA.

A flow diagram of the principal programs and subroutines is shown in figure 1. Program blocks appear in solid outline, input data sets in circular dashed outline and optional output in rectangular dashed outline. Input data blocks must be provided by the user and are given an alphabetic code. These are required in the following order depending on the option selection:

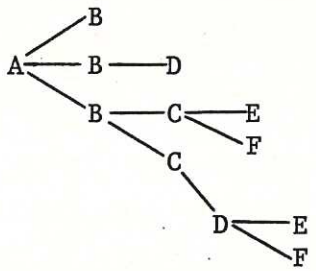

The complete list of card images for each alphabetic block specified above is given in Appendix (i) and details of input and output data streams in Appendix (ii).

5. Illustrative Examples

In this section, we demonstrate some of the ways in which the computer package may be used. The first objective is to illustrate the various options possible, such as selection of output and choice of ionisation model. The second is to discuss in more detail, for some test cases, the selection of atomic coefficients which are to be compiled in the data sets; and then to show the differences which might be caused either by using alternative sources or through uncertainties in the data. Titanium, oxygen and carbon, being important impurities in existing and prospective fusion devices, are suitable elements for the purpose. Table 1 shows the first page of program output, which reproduces the initial parameters, ion choice and basic plasma conditions selected in the data blocks A and B (Appendix (i)) provided by the user. JOPT4 selects the ionisation model. Figure 2 shows the equilibrium fractional abundances (JOPT4=2) for carbon ions, graphical and numerical output being obtained by setting JOPT8=4. The graphs are multicolour showing collisional dielectronic ionisation and recombination coefficients in addition to the fractional abundances, but these coefficients have been suppressed in figure 2 for clarity. The numerical tabulations of fractional abundances and collisional dielectronic coefficients are shown in tables 2 and 3. The special option of having an extended temperature range ionisation balance for a single electron density was used by setting MAXD=1 and MAXT≠MAXD in this case.

Figure 3 illustrates results for some titanium ions in time dependent ionisation (JOPT4=3). A number of curves have been superposed together with the temperature profile to show the behaviour with different evolution timescales. Graphical output alone is

selected by setting JOPT7=2. Figure 4 illustrates results for carbon ions in spatially non-equilibrium ionisation (JOPT4=4). Figure 5 shows the parameters used for the calculation of figure 4 and simulates recycling in a Tokamak section. Model calculations such as those shown in figures 3 and 4 require the data described in blocks E and F (Appendix (i)). In all these cases the ionisation and recombination data of Summers (cf. section 3.1) has been selected by setting JOPT5=JOPT6=1. This choice obviates the necessity of supplying data block D.

The further calculation of level populations, emissivities and theoretical spectra is controlled by parameters JOPT3, JOPT8 and JOPT9, together with cards 2,3 and 4 of data block A. Table 4 shows the excited level indexing, classification and energies generated by the codes. Tables 5 and 6 give sample output of excited populations and the emissivities of the various spectrum lines. Figure 8 shows the synthetic spectrum for Ti^{+13}-Ti^{+15} in the wavelength region 100-300Å at the electron temperature $T_e = 4 \times 10^6$ K. These results are for ionisation balance.

5.1 Titanium

We have considered the ionisation stages from Ti^{+13}(F-like) to Ti^{+19}(Li-like). Radiative and collisional atomic data for these titanium ions have recently been obtained by Bhatia et.al. (1980) with the well known University College London (UCL) codes. Since there appears to be no other source of readily available data we have used their transition probabilities and distorted wave collision strengths for electron impact excitation. Our treatment of electric quadrupole transitions that are induced by proton collisions differs however

from theirs. We have used the semi-classical method proposed by Bely and Faucher (1970) which was outlined in section 2.3 case (a). When ignoring the effect of protons, our results ought to agree with those of Bhatia et.al. since they solve the same set of statistical equilibrium equations as us. Any lack of agreement will presumably reflect differences in numerical techniques. Such a comparison is clearly of great use when developing a suite of programs as complicated as the present one.

Figure 6 shows the populations of excited levels of Ti^{+16} (C-like) as a function of electron density at the electron temperature $T_e = 6.5 \times 10^6$ ^oK. At $N_e = 10^{14} cm^{-3}$, our populations differ by <2% from those of Bhatia et.al. (1980). Our results were obtained using their theoretical energies although it is unclear whether they use theoretical or experimental energies in their computations. Since the proton density is set equal to zero, any discrepancies ought toreflect differences in the way rate coefficients are calculated from collision strengths. Bhatia et.al. gave collision strengths at only three energies for each transition and so there is considerable uncertainty in the quadrature over energy. The uncertainty is even greater at higher temperatures when high energy collision strengths obtained by extrapolation contribute significantly to the rates (see the discussion in section 2.2).

5.2 Oxygen (OVII)

In this section we take two different sources of collision strength data and compare the calculation of the populations of excited states of OVII for the n=3,2 and 1 shells.

The first source of data was obtained from the calculations of Sampson (1974a) for ions with one and two valence electrons. Using his prescriptions we obtained collision strengths of for the

n'=3,2-n=1,2 transitions in OVII.

In the second set of data Sampson's collision strengths were retained for the n'=3 - n=1,2 transitions, while for the n'=2 - n=1,2 transitions the distorted wave calculations of Pradhan et.al. (1981) were used. Note that these authors took into account the effects of autoionizing resonances on the cross-sections.

The transition probabilities employed in both sets of data were obtained from the atomic structure codes developed at University College London (Eissner et.al. 1974). The most intense spectral lines arise from the 2-1 transitions. A comparison of the population of the excited levels is shown in figure 7 for both sets of data. The differences due to the use of collision strength data can be seen from the figure where resonance effects are expected to account for large discrepancies in individual cases. The omission of 3-2,1 data produces a variation of up to 5% in the calculated values of the populations.

Acknowledgements

We wish to thank Dr. N.J. Peacock for many helpful discussions on this work. The research was supported by a grant from Culham Laboratory.

References

Alder K., Bohr R., Huus T., Mottleson B. and Winter A., 1956, Rev. Mod. Phys. 28, 432

Belling J.A., 1971, Ph.D. thesis, University College London.

Bely O., 1968, J. Phys. B: Atom Molec. Phys. 1, 23.

Bely O., Faucher P., 1970, Astron. and Astrophys., 6, 88.

Bhatia A.K., Feldman U. and Doschek G.A., 1980, J. Appl. Phys., 51, 1464.

Burgess A., 1964, Proc. Symp. Atomic Collision processes in plasmas, Culham report, Culham Laboratory, AERE-R4818.

Burgess A., Hummer D.G., and Tully J.A., 1970, Phil. Trans. 266, 225.

Burgess A., and Summers H.P., 1976, Mon. Not. R. astr. Soc., 174, 345.

Burgess A., Summers H.P., Cochrane D.M., and McWhirter R.W.P., 1977, Mon. Not. R. astr. Soc. 179, 275.

Burke P.G. and Seaton M.J., 1971, Methods in Computational Physics, 10, 1.

Crees M.A., Seaton M.J. and Wilson P.M.H., 1978, Comp. Phys. Commun. 15, 23.

Cowan R.D., 1968, J. Opt. Soc. Amer. 58, 808.

Cowan R.D. and Griffin D.C., 1976, J. Opt. Soc. Am., 66, 1010.

Eissner W., Jones M. and Nussbaumer, H., 1974, Comp. Phys. Commun. 8, 270.

Golden L.B., and Sampson D.H., (1977) J. Phys. B. 10, 2229.

Henry R.J.W., 1981, Phys. Rep., 68, 1.

Lotz W., 1967, Astrophys. J. Supple. 14, 207.

Landman D.A., and Brown T., 1979, Astrophys. J. 23, 636.

McWhirter R.W.P. and Summers H.P., 1982, Applications of Atomic Collision Physics, Vol II 'Fusion' Pub: Academic Press(to be published)

Parks A.D. and Sampson D.H., 1972, Ap. J., 178, 571.

Pradhan A.K., Norcross D.W. and Hummer D.G., 1981, Phys. Rev. A 23, 619.

Sahal - Brechot S., 1974, Astron. and Astrophys. 32, 147.

Sampson D.H., 1974, Astrophys. J. Suppl. 263, 309.

Seaton M.J., 1964, Planet Space Sci. Rev. 12, 55.

Summers H.P., 1974, Appleton Laboratory Report IM - 367.

APPENDIX (I)

BLOCK A. OPTION SELECTION

1. OPTION CARD.PARAMETERS:JOPT1,JOPT2,JOPT3,JOPT4,JOPT5,JOPT6,JOPT7,JOPT8,JOPT9,THRES
   FORMAT:9I5,D10.2

   WHERE JOPT1=(1 SELECT MAIN1
   (2 -NOT YET IMPLEMENTED
   JOPT2=(1 SELECT GENERAL Z X-SECT DATA - NOT YET IMPLEMENTED
   (2 " ELEMENT SPECIFIC X-SECT DATA
   JOPT3=(1 NO EXCITED LEVEL POPULATION OUTPUT
   (2 GRAPHICAL " " "
   (3 NUMERICAL " " "
   (4 GRAPH.+NUMER. " " "
   JOPT4=(1 SELECT NULL BALANCE, STAGE ABUNDANCES SET TO UNITY
   (2 SELECT ION3 IONISATION EQUILIBRIUM BALANCE
   (3 " ION4 IONISATION MODEL - TIME DEPENDENT
   (4 " ION5 IONISATION MODEL - SPATIAL - NOT YET IMPLEMENTED
   JOPT5=(1 SELECT IONISATION RATE COEFFICIENT ACCORDING TO SPECS. OF SECTION 3.1.1 - SCD WITHOUT AUTO IONISATION
   (2 - SCD WITH AUTO IONISATION
   (3 - S (ECIP DIRECT ONLY WITH DATA
   (4 - S (SEF DIPECT ONLY WITH DATA
   (5 - SCD (WITH ECIP FOR DIRECT)
   (6 - SCD (WITH SEF FOR DIRECT)
   JOPT6=(1 SELECT RECOMBINATION RATE COEFFICIENT ACCORDING TO SPECS. OF SECTION 3.1.2 - ACD
   (2 - ACD (WITH SCALING FACTOR)
   JOPT7=(1 NO IONISATION STAGE ABUNDANCE OUTPUT
   (2 GRAPHICAL " " "
   (3 NUMERICAL " " "
   (4 GRAPH.+NUMER. " " "
   JOPT8=(1 NO EMISSIVITY OUTPUT
   (2 GRAPHICAL "
   (3 NUMERICAL "
   (4 GRAPH.+NUMER. "
   JOPT9=(-1 ALL LEVEL POPULATIONS OF SELECTED IONISATION STAGES ARE OUTPUT
   (N WITH N.GE.0. FIRST N LEVEL POPULATIONS ARE OUTPUT. IF N EXCEEDS TOTAL NUMBER OF
   LEVELS FOR AN IONISATION STAGE, THEN ALL ARE OUTPUT
   THRES=THRESHOLD FOR EMISSIVITY GRAPHING AND TABULATION

2. OUTPUT CARD, TEMPERATURE SET.
   PARAMETERS:(ITR(I),I=1,NTR)
   FORMAT:10I5

   WHERE ITR(I)=INDEX OF TEMPERATURES FOR GRAPHICAL EMISSIVITY AND TABULAR LEVEL POPULATION OUTPUT
   FROM THE TEMPERATURE ARRAY TEA. THE ASSOCIATED TEMPERATURE IS TEA(ITR(I))
   NOTE ITR(I).LE.MAXT (SEE BLOCK B)

3. OUTPUT CARD, WAVELENGTH REGIONS.
   PARAMETERS:(IWR(I),I=1,NWR)
   FORMAT:6I5

   WHERE IWR(I)=INDEX OF WAVELENGTH REGIONS FOR GRAPHICAL EMISSIVITY OUTPUT FROM WAVELENGTH REGION SET.
   NAMELY 1. 0-25A
   2. 25-100A
   3. 100-300A
   4. 300-1200A
   5. 1200-3000A

```
            6. 3000-6500A
        NOTE IWR(I).LE.6.


  4. OUTPUT CARD, IONISATION STAGE SET.
                PARAMETERS:(IZR(I),I=1,NZR)
                    FORMAT:6I5

        WHERE IZR(I)=ION CHARGE+1 OF ITH STAGE WHOSE LEVEL POPULATIONS ARE TO BE OUTPUT
        NOTE NUMBER OF LEVEL POPULATIONS OUTPUT FOR EACH IONISATION STAGE IS CONTROLLED BY JOPT9
-------------------------------------------------------------------------------------------------

BLOCK B.

  1. ION SPECIFICATION
                PARAMETERS:(ELTIT(I),I=1,5),IZ0,IZE1,IZE2
                    FORMAT:5A3,3I5

        WHERE ELTIT=ELEMENT TITLE
               IZ0=ATOMIC NUMBER
              IZE1=ION CHARGE OF FIRST STAGE TO BE INCLUDED
              IZE2=ION CHARGE OF LAST STAGE TO BE INCLUDED


  2. NUMBER OF DENSITY AND TEMPERATURE VALUES
                PARAMETERS:MAXT,MAXD
                    FORMAT:2I5

        WHERE  MAXD=NUMBER OF ELECTRON/PROTON DENSITIES
               MAXT=NUMBER OF ELECTRON/PROTON TEMPERATURES

        REQUIRE 1.LE.MAXD.LE.10 , AND MAXT.EQ.MAXD
           OR   1.LE.MAXT.LE.40 , AND MAXD EQ.1

  3. ELECTRON TEMPERATURES
                PARAMETERS:(TEA(I),I=1,MAXT)
                    FORMAT:8D10.2

  4. PROTON TEMPERATURES
                PARAMETERS:(TPA(I),I=1,MAXT)
                    FORMAT:8D10.2

  5. ELECTRON DENSITIES
                PARAMETERS:(DENSA(I),I=1,MAXD)
                    FORMAT:8D10.2

  6. PROTON DENSITIES
                PARAMETERS:(DENSPA(I),I=1,MAXD)
                    FORMAT:8D10.2

-------------------------------------------------------------------------------

BLOCK C.  SPATIAL OR TIME DEPENDENT MODELS

  1. INDEPENDENT COORDINATE VALUES
               PARAMETERS:(X(I),I=1,MAXT)
                   FORMAT:8D10.2

        BLOCK REQUIRED ONLY IF JOPT4=3 OR 4
        IF JOPT4=3, X-VALUES ARE TIMES
        IF JOPT4=4, X-VALUES ARE RADIAL POSITIONS
        CORRESPONDING TO THE TEMPERATURES AND DENSITIES OF BLOCK B.

  2. VELOCITY FIELD
               PARAMETERS:(V(I),I=1,MAXT)
```

```
                    FORMAT:6D10.2

        CARD REQUIRED ONLY IF JOPT4=4

-------------------------------------------------------------------------------

BLOCK D.  IONISATION AND RECOMBINATION RATE ADJUSTMENT.

          THIS BLOCK IS REQUIRED ONLY IF JOPT6.NE.2 AND JOPT5.NE.1,2

  1. NUMBER OF STAGES FOR MODIFICATION
               PARAMETERS:NSTAGE
                   FORMAT:I5

        WHERE NSTAGE=NUMBER OF STAGES TO BE MODIFIED
              NSTAGE=0 OR BLANK IMPLIES NO FUPTHER CARDS IN THIS BLOCK

        REQUIRE NSTAGE.LE.IZE2-IZE1+1

  2. SUCCESSIVE CARD PAIRS FOR EACH STAGE
         (A)  PARAMETERS:IZ,NS,NA
                         (EION(I),ZETA(I),I=1,NS)
                   FORMAT:3I5,6D10.2
         (B)  PARAMETERS:SRF,(EA(I),QA(I),I=1,NA)
                   FORMAT:5X,7D10.2

        WHERE IZ=CHARGE OF IONISATION STAGE
              NS=NUMBER OF SHELLS TO BE TAKEN INTO ACCOUNT
              NA=NUMBER OF DISTINCT AUTOIONISING LEVELS
              ZETA=NUMBER OF ELECTRONS IN SHELL
              SRF=SCALING FACTOR OF RECOMBINATION RATE TO THIS STAGE
              EA=EXCITATION ENERGIES OF AUTOIONISING LEVELS
              QA=THRESHOLD CROSS-SECTIONS OF AUTOIONISING LEVELS

-------------------------------------------------------------------------------

BLOCK E.  SPATIALLY INHOMOGENEOUS MODEL PARAMETERS

  1. DIFFUSION PARAMETERS:P,A,B,C,D
                   FORMAT:5D10.2

        WHERE P=N(Z)
              A=A(Z)
              B=B(Z)
              C=C(Z)
              D=D(Z)    SEE SECTION 3.3
        WITH A CARD REQUIRED FOR EACH INCLUDED IONISATION STAGE FROM IZE1 TO IZE1 TO IZE2

        NOTE THIS DATA BLOCK IS ONLY REQUIRED IF JOPT4=4

-------------------------------------------------------------------------------

BLOCK F.  TIME DEPENDENT MODEL PARAMETERS.

  1. INITIAL FRACTIONAL ABUNDANCES
                PARAMETERS:P
                    FORMAT:D10.2

        WHERE P=FRACTIONAL STAGE ABUNDANCE AT INITIAL TIME
        WITH A CARD REQUIRED FOR EACH INCLUDED IONISATION STAGE FROM IZE1 TO IZE2

        NOTE THIS DATA BLOCK IS ONLY REQUIRED IF JOPT4=3

-------------------------------------------------------------------------------
```

Appendix (ii)

A number of input and output data streams, and associated data sets must be provided. These are as follows:

Stream	In/Out	Data Files
5	IN	User data (Appendix (i))
6	OUT	Ionisation stage fractional abundances and excited ion level energies and classification
7	OUT	Diagnostic data
9	IN	PROTDAT
10	IN	Atomic data compilation for element, e.g. TITANIUM
11	IN	IPAXDATA
13	OUT	Level populations
14	OUT	Emissivities
16	IN/OUT	Temporary direct access file
17	IN/OUT	Temporary direct access file
50	OUT	Graphical output file

Table 1

Initial parameter table.

```
                COPASE PROGRAM - USER PARAMETER SPECIFICATION

  JOPT1      JOPT2      JOPT3      JOPT4      JOPT5      JOPT6      JOPT7      JOPT8      JOPT9      THRES
    1          2          1          2          1          1          4          1         10       5.00D 01
0OUTPUT TEMPERATURE SELECTION
  ITR(I),I=1,NTR
    1          2
0OUTPUT WAVELENGTH RANGE SELECTION
  IWR(I),I=1,IWR
    3          5
0OUTPUT IONISATION STAGE SELECTION
  IZR(I),I=1,NZR
    1          3
    ELEMENT                IZ0        IZE1       IZE2
 CARBON                     6          0          6


    ELECTRON TEMPERATURES
  5.00D 03  6.00D 03  7.00D 03  8.00D 03  9.00D 03  1.00D 04  1.26D 04  1.59D 04
  2.00D 04  3.00D 04  4.00D 04  5.00D 04  6.00D 04  7.00D 04  8.00D 04  9.00D 04
  1.00D 05  1.26D 05  1.59D 05  2.00D 05  3.00D 05  4.00D 05  5.00D 05  6.00D 05
  7.00D 05  8.00D 05  9.00D 05  1.00D 06  1.26D 06  1.59D 06  2.00D 06  3.00D 06
  4.00D 06  5.00D 06  6.00D 06  7.00D 06  8.00D 06  9.00D 06  1.00D 07
    PROTON TEMPERATURES
  5.00D 03  6.00D 03  7.00D 03  8.00D 03  9.00D 03  1.00D 04  1.26D 04  1.59D 04
  2.00D 04  3.00D 04  4.00D 04  5.00D 04  6.00D 04  7.00D 04  8.00D 04  9.00D 04
  1.00D 05  1.26D 05  1.59D 05  2.00D 05  3.00D 05  4.00D 05  5.00D 05  6.00D 05
  7.00D 05  8.00D 05  9.00D 05  1.00D 06  1.26D 06  1.59D 06  2.00D 06  3.00D 06
  4.00D 06  5.00D 06  6.00D 06  7.00D 06  8.00D 06  9.00D 06  1.00D 07
    ELECTRON DENSITIES
  1.00D 13
    PROTON DENSITIES
  0.00D 00
```

Table 2

Equilibrium fractional abundances for carbon ions, electron density Ne = 10^{13} cm^{-3}.

CARBON LOG(NE)= 13.00

	-LOG(N(Z)/NTOT)							
	Z=	Z=	Z=	Z=	Z=	Z=	Z=	ZM
LOG(TE)	0	1	2	3	4	5	6	
3.7	0.000	7.202						0.000
3.8	0.000	5.126						0.000
3.8	0.000	3.616						0.000
3.9	0.001	2.477						0.003
4.0	0.011	1.605						0.025
4.0	0.051	0.952						0.112
4.1	0.499	0.165	6.698					0.683
4.2	1.291	0.023	4.450					0.949
4.3	1.994	0.005	2.801					0.991
4.5	3.067	0.073	0.815	6.254				1.152
4.6	4.005	0.451	0.190	3.562	9.301			1.646
4.7	4.838	0.926	0.058	2.157	6.192			1.888
4.8	5.487	1.327	0.046	1.269	4.152			2.007
4.8	6.041	1.697	0.110	0.694	2.743			2.186
4.9	6.581	2.090	0.265	0.365	1.778			2.457
5.0	7.129	2.517	0.496	0.219	1.130			2.749
5.0	7.677	2.960	0.775	0.199	0.701			3.029
5.1	9.054	4.114	1.600	0.477	0.193			3.616
5.2		5.363	2.555	0.997	0.047			3.894
5.3		6.497	3.431	1.523	0.013	8.202		3.969
5.5		8.126	4.662	2.262	0.002	4.648		3.995
5.6		8.986	5.272	2.583	0.002	2.834	7.626	3.999
5.7		9.521	5.623	2.730	0.008	1.763	5.194	4.015
5.8		9.908	5.866	2.815	0.037	1.098	3.604	4.079
5.8			6.074	2.894	0.102	0.688	2.519	4.210
5.9			6.276	2.988	0.205	0.447	1.764	4.391
6.0			6.480	3.098	0.336	0.320	1.229	4.596
6.0			6.689	3.225	0.490	0.272	0.850	4.816
6.1			7.269	3.630	0.959	0.380	0.325	5.363
6.2			7.990	4.185	1.560	0.698	0.112	5.744
6.3			8.740	4.782	2.156	1.065	0.042	5.900
6.5				5.806	3.093	1.650	0.010	5.976
6.6				6.480	3.671	1.991	0.005	5.989
6.7				6.970	4.078	2.220	0.003	5.994
6.8				7.351	4.386	2.389	0.002	5.996
6.8				7.661	4.633	2.521	0.001	5.997
6.9				7.923	4.839	2.630	0.001	5.998
7.0				8.147	5.013	2.722	0.001	5.998
7.0				8.344	5.164	2.800	0.001	5.998

Table 3

Collisional dielectronic recombination and ionisation coefficients for carbon ions, electron density Ne = 10^{13} cm^{-3}.

Z= 4 LOG NE / LOG TE	-LOG ALPHA 13.00	-LOG S 13.00
3.70	10.373	
3.78	10.432	
3.85	10.481	
3.90	10.523	
3.95	10.561	
4.00	10.595	
4.10	10.669	
4.20	10.743	
4.30	10.816	
4.48	10.946	
4.60	11.038	
4.70	11.109	
4.78	11.167	
4.85	11.217	
4.90	11.259	
4.95	11.297	
5.00	11.331	
5.10	11.404	
5.20	11.479	
5.30	11.55819.746	
5.48	11.71516.360	
5.60	11.81714.649	
5.70	11.85813.612	
5.78	11.85412.915	
5.85	11.82712.413	
5.90	11.79112.033	
5.95	11.75211.736	
6.00	11.71311.496	
6.10	11.62511.047	
6.20	11.54510.683	
6.30	11.48610.395	
6.48	11.45710.014	
6.60	11.499 9.819	
6.70	11.559 9.701	
6.78	11.619 9.622	
6.85	11.677 9.565	
6.90	11.732 9.523	
6.95	11.782 9.490	
7.00	11.829 9.464	

Z= 5 LOG NE / LOG TE	-LOG ALPHA 13.00	-LOG S 13.00
3.70	10.145	
3.78	10.206	
3.85	10.258	
3.90	10.302	
3.95	10.342	
4.00	10.377	
4.10	10.455	
4.20	10.533	
4.30	10.610	
4.48	10.746	
4.60	10.842	
4.70	10.917	
4.78	10.978	
4.85	11.030	
4.90	11.075	
4.95	11.114	
5.00	11.150	
5.10	11.227	
5.20	11.305	
5.30	11.382	
5.48	11.51918.529	
5.60	11.61616.407	
5.70	11.69115.123	
5.78	11.75314.259	
5.85	11.80613.638	
5.90	11.85113.168	
5.95	11.89212.801	
6.00	11.92812.505	
6.10	12.00011.951	
6.20	12.06811.503	
6.30	12.16911.146	
6.48	12.31610.676	
6.60	12.42210.436	
6.70	12.50610.289	
6.78	12.57710.190	
6.85	12.63910.119	
6.90	12.69510.066	
6.95	12.74510.025	
7.00	12.791 9.992	

Table 4

Excited level index, classification and energies for Ti^{+14} and Ti^{+15}.

ION	Z0	Z1	ION.POT.(W.NO.)		
TI+14	22	15	7593000.		
ENERGY LEVELS					
INDEX	CONFIG.	(2S+1)L(J)	W.NO.	B.W.NO.	ENER.(RYD)
1	2S2 2P4	(3)1(2.0)	.0.	7593000.	0.0000000
2	2S2 2P4	(3)1(1.0)	39400.	7553600.	0.3590400
3	2S2 2P4	(3)1(0.0)	42500.	7550500.	0.3872893
4	2S2 2P4	(1)2(2.0)	109050.	7483950.	0.9937388
5	2S2 2P4	(1)0(0.0)	215950.	7377050.	1.9678854
6	2S1 2P5	(3)1(2.0)	712300.	6880700.	6.4909691
7	2S1 2P5	(3)1(1.0)	742900.	6850100.	6.7698174
8	2S1 2P5	(3)1(0.0)	762200.	6830800.	6.9456923
9	2S1 2P5	(1)1(1.0)	978350.	6614650.	8.9154003
10	2P6	(1)0(0.0)	1656550.	5936450.	15.0956266
ION	Z0	Z1	ION.POT.(W.NO.)		
TI+15	22	16	8440000.		
ENERGY LEVELS					
INDEX	CONFIG.	(2S+1)L(J)	W.NO.	B.W.NO.	ENER.(RYD)
1	2S2 2P3	(4)0(1.5)	0.	8440000.	0.0000000
2	2S2 2P3	(2)2(1.5)	114400.	8325600.	1.0424917
3	2S2 2P3	(2)2(2.5)	129000.	8311000.	1.1755370
4	2S2 2P3	(2)1(0.5)	196100.	8243900.	1.7869985
5	2S2 2P3	(2)1(1.5)	217800.	8222200.	1.9847439
6	2S1 2P4	(4)1(2.5)	589100.	7850900.	5.3682857
7	2S1 2P4	(4)1(1.5)	620500.	7819500.	5.6544241
8	2S1 2P4	(4)1(0.5)	633700.	7806300.	5.7747117
9	2S1 2P4	(2)2(1.5)	811500.	7628500.	7.3949479
10	2S1 2P4	(2)2(2.5)	815500.	7624500.	7.4313987
11	2S1 2P4	(2)0(0.5)	938300.	7501700.	8.5504370
12	2S1 2P4	(2)1(1.5)	975100.	7464900.	8.8857840
13	2S1 2P4	(2)1(0.5)	1019100.	7420900.	9.2867424
14	2P5	(2)1(1.5)	1536000.	6904000.	13.9970918
15	2P5	(2)1(0.5)	1586300.	6853700.	14.4554601

Table 5

Excited level populations for Ti^{+15}. Electron temperature, $Te = 4 \times 10^6$ °K, electron density, $Ne = 10^{13}$ cm^{-3}.

POPULATIONS ZI = 16 TE = 4.00D 06 NE = 1.00D 13

INDEX	CONFIG.	(2S+1)L(J)	W.NO.	POP(I,KSTCK)
2	2S2 2P3	(2)2(1.5)	114400.	2.55D-01
3	2S2 2P3	(2)2(2.5)	129000.	4.61D-01
4	2S2 2P3	(2)1(0.5)	196100.	6.17D-02
5	2S2 2P3	(2)1(1.5)	217800.	6.78D-02
6	2S1 2P4	(4)1(2.5)	589100.	6.22D-07
7	2S1 2P4	(4)1(1.5)	620500.	3.42D-07
8	2S1 2P4	(4)1(0.5)	633700.	1.63D-07
9	2S1 2P4	(2)2(1.5)	811500.	5.46D-08
10	2S1 2P4	(2)2(2.5)	815500.	9.37D-08
11	2S1 2P4	(2)0(0.5)	938300.	1.28D-08
12	2S1 2P4	(2)1(1.5)	975100.	3.16D-08
13	2S1 2P4	(2)1(0.5)	1019100.	4.44D-09
14	2P5	(2)1(1.5)	1536000.	1.45D-10
15	2P5	(2)1(0.5)	1586300.	5.15D-11

Table 6

Emissivities and wavelength of spectrum lines for titanium ions Ti^{+13} – Ti^{+15}. Index references are to listings on Table 4. Results are for ionisation equilibrium.

SPECTRUM LINE WAVELENGTHS AND EMISSIVITIES TE = 4.00D 06 NE = 1.00D 13

ION	INDEX1	INDEX2	WVLN(A)	EMIS
13	2	1	2114.1649	4.343D 02
13	3	2	129.4331	1.128D 03
14	4	1	917.0105	1.125D 02
14	7	1	134.6076	3.052D 02
14	7	2	142.1464	1.508D 02
14	7	3	142.7756	1.897D 02
15	6	1	169.7505	1.270D 02
13	3	1	121.9661	2.679D 05
14	2	1	2538.0711	8.741D 01
14	6	1	140.3903	9.107D 02
14	6	2	148.6105	2.690D 02
14	8	2	138.3509	1.756D 02
14	9	4	115.0351	3.402D 02
15	7	1	161.1604	8.294D 01

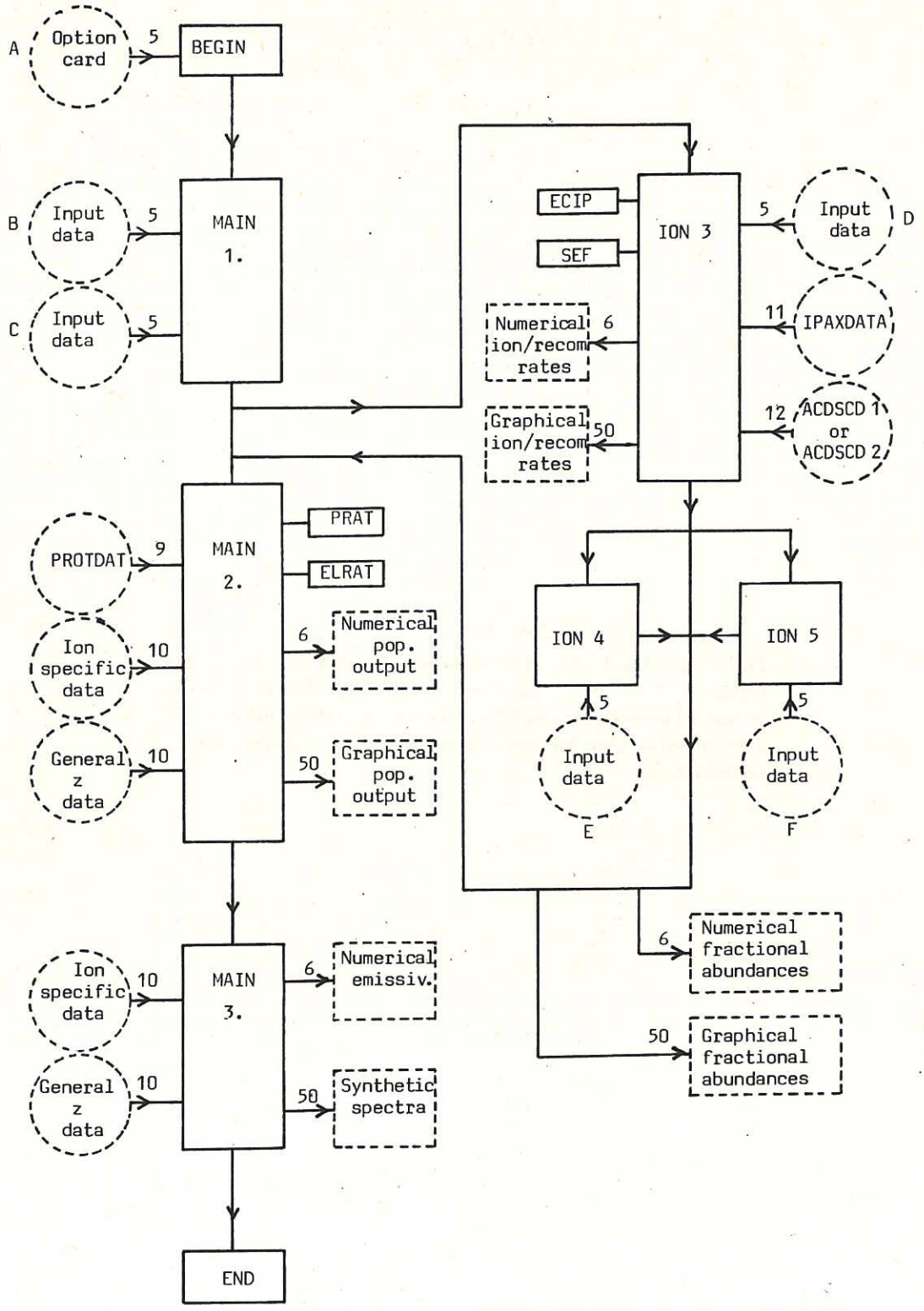

Fig.1 Flow diagram of principal program units and data sets. Sub programs are in solid outline, optional user output in square dashed outline, input data in circular dashed outline.

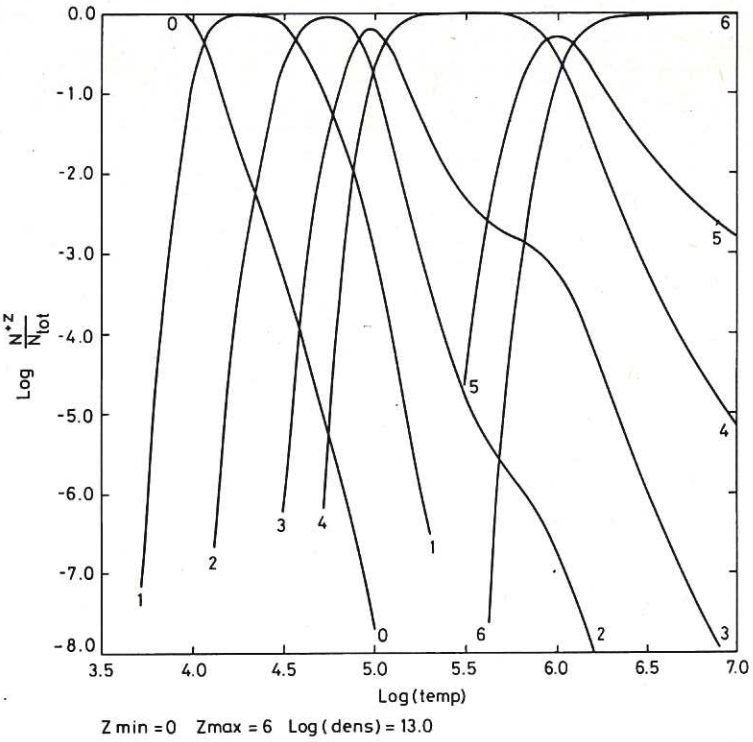

Fig.2 Equilibrium fractional abundances for carbon ions. Electron density $N_e = 10^{13}$ cm^{-3}. The computer programs also superimpose collisional dielectronic recombination and ionisation coefficients in multi colour plots but this is suppressed here for clarity in reproduction.

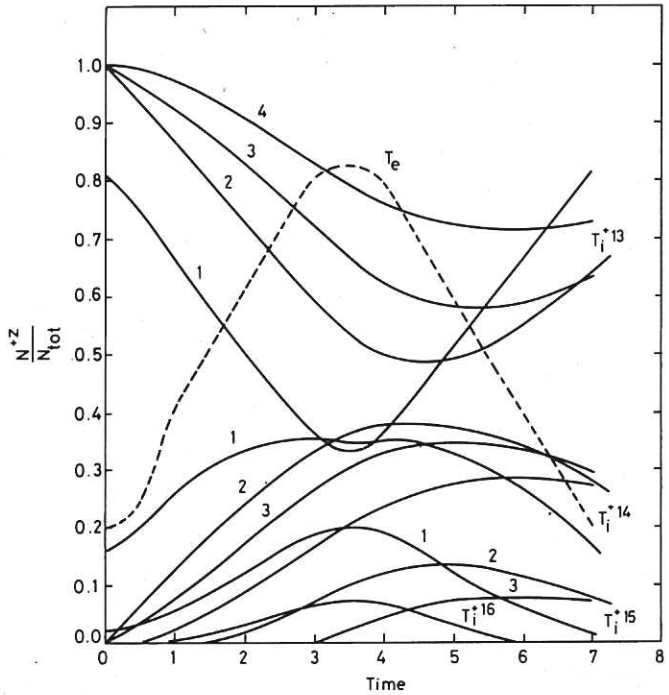

Fig.3 Time dependent fractional abundances for the Titanium ions T_i^{+13} - T_i^{+16}. Electron density $N_e = 10^{13}$ cm^{-3}, with initial conditions $\frac{N(T_i^{+13})}{N_{tot}} = 1$ at time t = 0.

Electron temperature profile shown in dashed outline.

1. **Ionisation equilibrium abundances.**
2. **Unit of time on x-axis = 10^{-3} sec.**
3. **" " " " " = 0.5×10^{-3} sec.**
4. **" " " " " = 0.25×10^{-3} sec.**

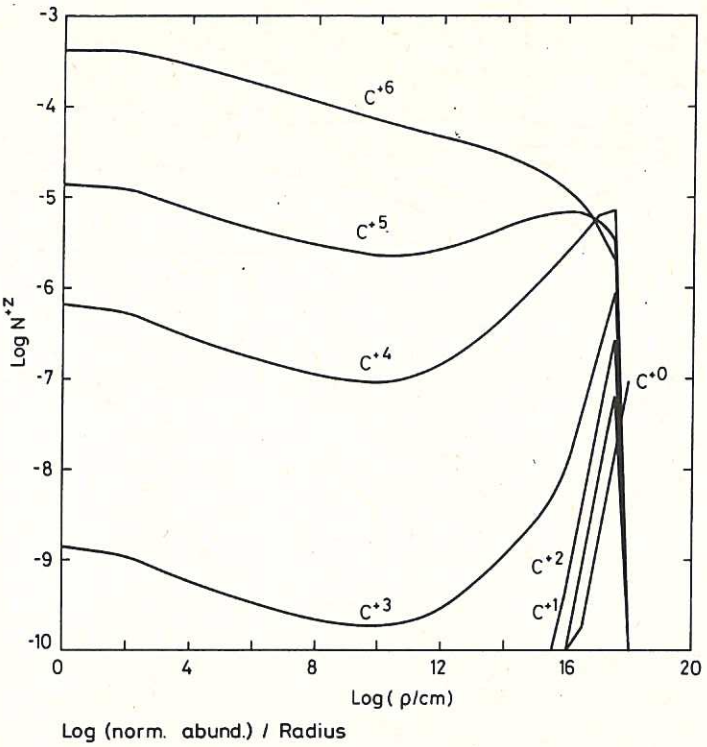

Fig.4 Abundances of carbon ions in spatially non-equilibrium model of recycling in a Tokamak section. Entry at plasma periphery is as neutral carbon. Abundances are normalised to unit neutral entry flux.

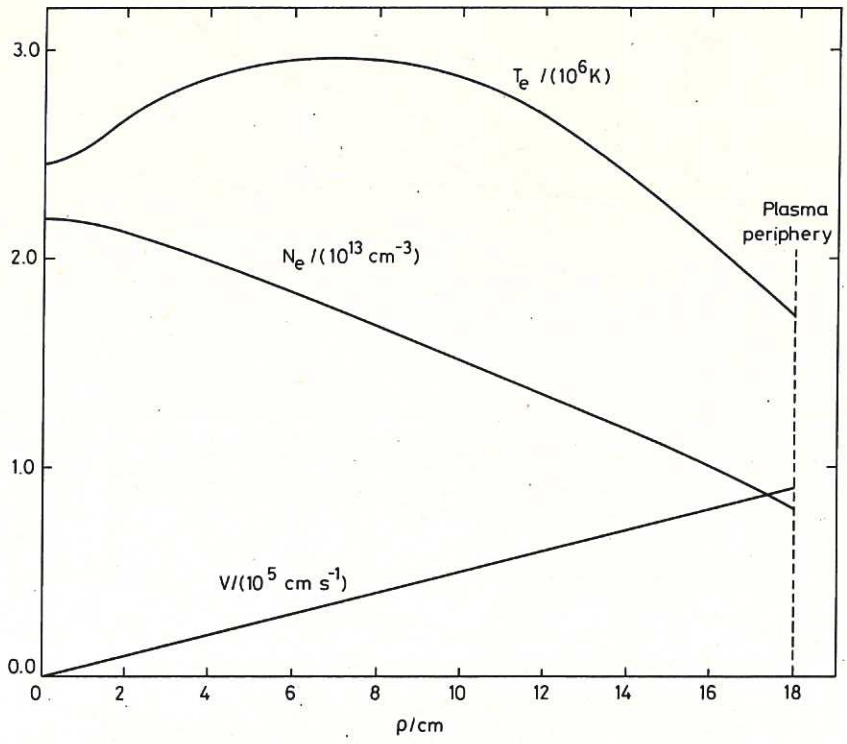

Fig.5 Electron temperature, electron density and neutral injected velocity profiles as a function of radius for results of figure 4.

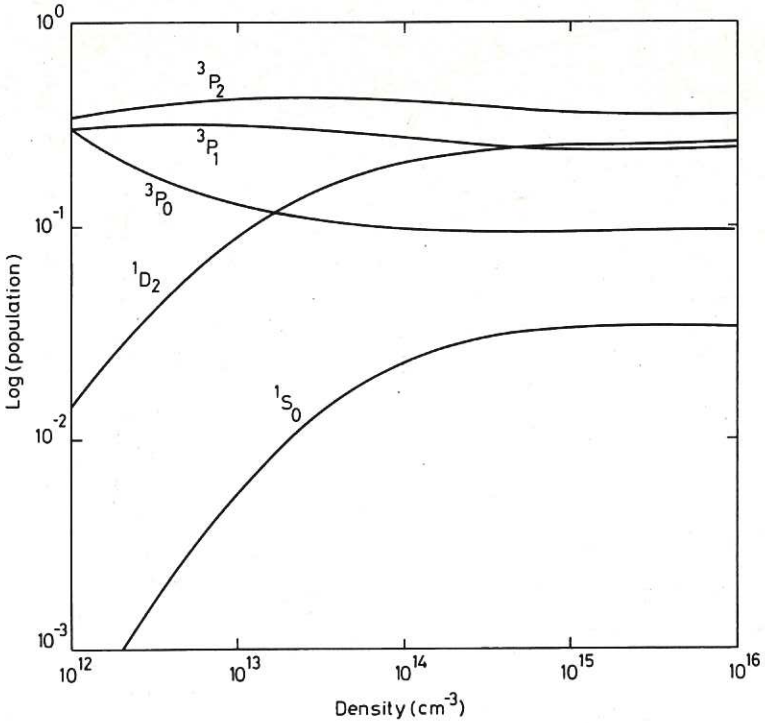

Fig.6 Dependence of populations of some excited levels of T_i^{+16} on electron density for electron temperature $T_e = 6.5 \times 10^6$ °K.

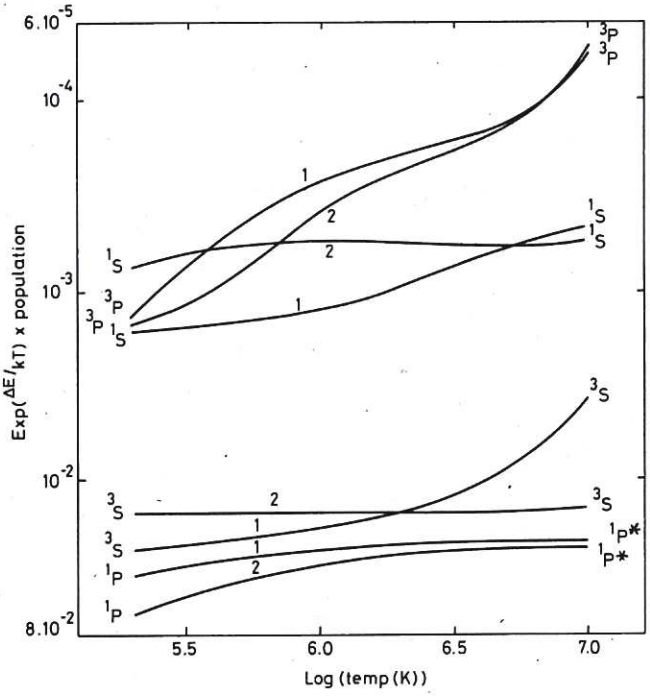

Fig.7 Dependence of populations of excited levels of 0^{+6} on temperature for electron density $N_e = 10^{13}$ cm^{-3}.
Curves show the influence of different collision strength data and the effect of omission of higher levels.

1. **Pradhan et al. (1981) data for n = 1, 2 - n^1 = 2; Sampson (1974) data for n = 1, 2 - n^1 = 3.**
2. **Sampson (1974) data for n = 1, 2 - n^1 = 2,3. Curves marked * are scaled. The ordinate is 2.58×10^6 exp($\Delta E/kT$) $\times$ population + 2.0×10^{-2}. ΔE is the energy of excited level above the ground level.**

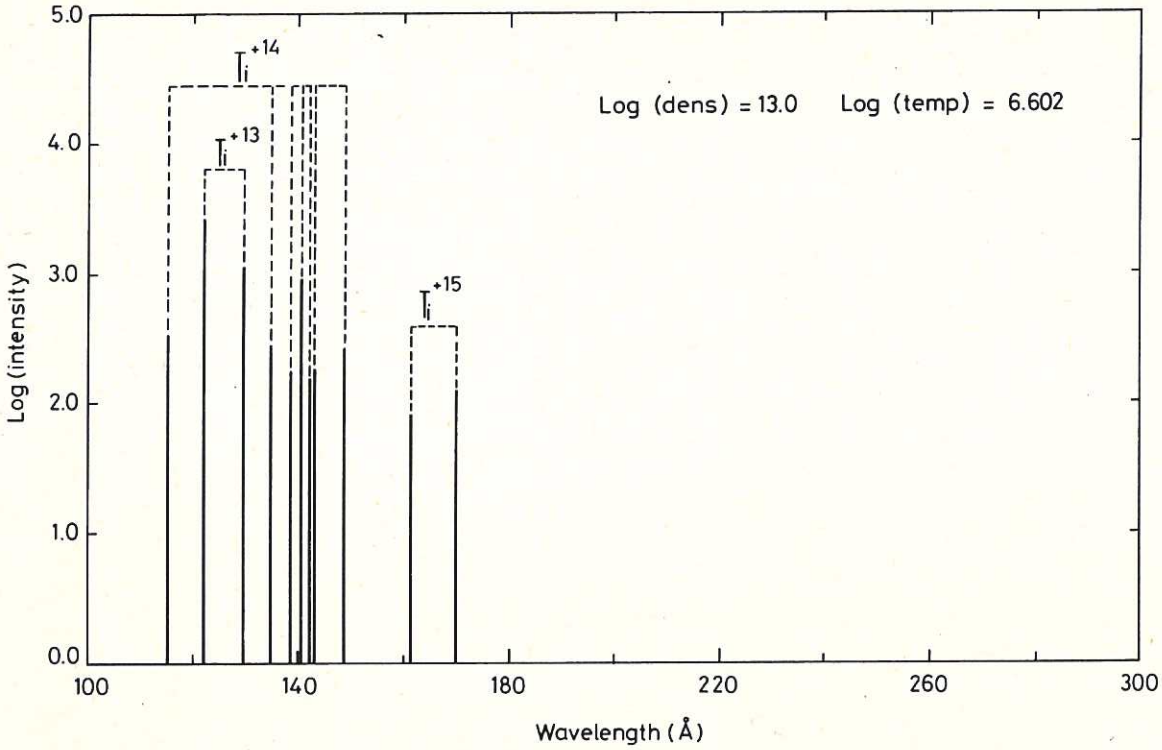

Fig.8 Synthetic spectrum for some titanium ions. Electron temperature, $T_e = 5 \times 10^6$ °K, electron density, $N_e = 10^{13}$ cm^{-3}, wavelength region 100–300 Å selected.

HER MAJESTY'S STATIONERY OFFICE

Government Bookshops

49 High Holborn, London WC1V 6HB
(London post orders: PO Box 569, London SC1 9NH)
13a Castle Street, Edinburgh EH2 3AR
41 The Hayes, Cardiff CF1 1JW
Brazennose Street, Manchester M60 8AS
Southey House, Wine Street, Bristol BS1 2BQ
258 Broad Street, Birmingham B1 2HE
80 Chichester Street, Belfast BT1 4JY

Publications may also be ordered through any bookseller